HHS Public Access

Author manuscript

Nat Chem Biol. Author manuscript; available in PMC 2011 December 01.

Published in final edited form as:

Nat Chem Biol. 2011 June ; 7(6): 351–358. doi:10.1038/nchembio.558.

Temperature-dependent STIM1 activation induces Ca^{2+} influx and modulates gene expression

Bailong Xiao[1], **Bertrand Coste**[1], **Jayanti Mathur**[2], and **Ardem Patapoutian**[1,2,3]

[1]Department of Cell Biology, The Scripps Research Institute, La Jolla, CA 92037

[2]Genomics Institute of the Novartis Research Foundation, San Diego, CA 92121

Abstract

Intracellular Ca^{2+} is essential for diverse cellular functions. Ca^{2+} entry into many cell types including immune cells is triggered by depleting endoplasmic reticulum (ER) Ca^{2+}, a process termed store-operated Ca^{2+} entry (SOCE). STIM1 is an ER Ca^{2+} sensor. Upon Ca^{2+} store depletion, STIM1 clusters at ER-plasma membrane junctions where it interacts with and gates Ca^{2+}-permeable Orai1 ion channels. Here we show that STIM1 is also activated by temperature. Heating cells caused clustering of STIM1 at temperatures above 35°C without depleting Ca^{2+} stores, and led to STIM1/Orai1-mediated Ca^{2+} influx as a heat off-response (response after cooling). Interestingly, the functional coupling of STIM1 and Orai1 is prevented at high temperatures, potentially explaining the heat off-response. Importantly, physiologically-relevant temperature shifts modulates STIM1-dependent gene expression in Jurkat T-cells. Therefore, temperature is an important regulator of STIM1 function.

Introduction

Ca^{2+} entry through store-operated channels (SOC) drives diverse biological processes such as Ca^{2+} homeostasis, gene expression, cell differentiation, and secretion1. These channels open in response to depletion of ER Ca^{2+} upon activation of phospholipase C (PLC)-coupled receptors. The best characterized SOC are the calcium release-activated calcium (CRAC) channels2. CRAC channels play vital roles in T cells and other immune cells. They induce sustained Ca^{2+} influx, activate Ca^{2+}-dependent transcription factors such as nuclear factor of activated T cells (NFAT), and consequently initiate gene expression critical for inflammatory responses3,4. Defects in CRAC channel function have been associated with severe combined immunodeficiency5.

The molecular nature of CRAC channels had been a mystery over two decades until the recent identification of STIM1 and Orai16,7,8. STIM1 functions as the ER Ca^{2+}

[3]To whom correspondence should be addressed, apatapou@gnf.org.

Author Contributions: B.X. performed the bulk of the studies. B.C. performed all the electrophysiological studies. J. M. performed qRT-PCR, molecular cloning experiments. B.X., B.C., and A.P. designed the experiments and wrote the paper. All authors read and discussed the paper.

Competing Financial Interests: The authors declare no competing financial interests.

sensor9,10,11, while Orai1 serves as the pore-forming subunit at the plasma membrane2. STIM1 is a single transmembrane ER protein and detects ER Ca^{2+} through its amino-terminal EF-hand motif9,10. ER Ca^{2+} depletion causes partial unfolding of the EF-hand and sterile α motif (SAM) domains and oligomerization of STIM112,13. STIM1 then translocates to and clusters at ER-plasma membrane (PM) junctions7,10,14 where it ultimately gates Orai1 ion channels through direct binding15,16,17.

Temperature is an important regulator of immune cell function18,19,20,21. Immune cells can experience dramatic temperature change under either normal or pathophysiological conditions. For example, lymphocytes experience wide temperature variations while they circulate from central organs such as the spleen (37°C) to peripheral locations such as the skin (33°C or lower dependent on ambient temperature)22. In addition, lymphocytes – and indeed all cell types – are exposed to changing temperatures in situations of hypothermia, hyperthermia, or fever, when the core body temperature can rise up to 41°C. However, surprisingly little is known about the molecules used by immune cells to sense temperature variations. In thermosensitive Dorsal Root Ganglion (DRG) neurons, a subset of the Transient Receptor Potential (TRP) family of ion channels dubbed thermoTRPs is activated by distinct temperatures23,24. Some studies suggest that STIM1 interacts with TRP ion channels25 (but also see26). We tested if STIM1 can modulate thermoTRPs. Unexpectedly, we found that STIM1 itself is activated by changes in temperature alone, leading to Orai1-mediated Ca^{2+} influx.

Results

STIM1 and Orai1 mediate a unique heat response

We tested whether STIM1 modulates thermoTRPs such as warm-activated TRPV3 ion channels. Unexpectedly, we found that human embryonic kidney (HEK293T) cells transiently-transfected with STIM1 and Orai1 (STIM1/Orai1) alone showed robust Fluo-3 (a Ca^{2+} sensitive dye) responses upon heating to 39°C or 50°C. These responses were quantitatively equivalent to the heat responses of TRPV3-transfected cells, but mainly occurred during the cooling phase as the temperature cooled below 37°C (defined here as heat off-responses - responses after cooling) (Fig. 1a and Supplementary Results, Supplementary Fig. 1a). The STIM1-dependent heat off-responses were abolished by extracellular Ca^{2+} chelation (Supplementary Fig. 1b), suggesting Ca^{2+} influx rather than release from stores. This off-response was also present in STIM1 alone-transfected cells when heated to the higher temperature (Fig. 1a and Supplementary Fig. 1a), but absent in both vector-and Orai1-only transfected cells (Fig. 1a and Supplementary Fig. 1a). Multiple heating pulses evoked repeated heat off-responses in STIM1/Orai1-transfected cells, demonstrating recovery and reproducibility (Supplementary Fig. 1c). Similar to HEK cells, we observed heat off-responses in HeLa cells transfected with STIM1/Orai1 or STIM1 alone using single cell Ca^{2+} imaging (Fig. 1b and Supplementary Fig. 1d). The average intracellular Ca^{2+} concentration during the heat off-response reached up to 750 nM in STIM1/Orai1-transfected HeLa cells, matching a mono-exponential decay with a τ (time constant for the decay) of 380 s (Supplementary Fig. 1d). This suggests that heat is a robust stimulus in eliciting long-lasting Ca^{2+} increase in these cells. Furthermore, single cell

analysis from Fig. 1b revealed that the heat offresponses of most responding cells started to occur at the temperature of ~37°C (Fig. 1b, green trace), with a small portion of cells showing delayed responses even after cooling back to 25°C (Supplementary Fig. 1e). The heat off-response was blocked with either 2-aminoethoxydiphenyl borate (2-APB), a non-specific CRAC channel blocker (Supplementary Fig. 1f), or N-[5-(2-Chloro-5-trifluoro-methyl-phenyl)-pyrazin-2-yl]-2,6-difluoro-benzamice (Synta1), a putative selective CRAC channel blocker27 (Supplementary Fig. 1g–j), consistent with the requirement of STIM1/Orai1 for the response. RNAi experiments indicate that endogenous Orai1 mediated the heat off-response in STIM1 alone-transfected HeLa cells (Fig. 1c and Supplementary Fig. 1k, l). Although all proteins including ion channels can be modulated to some degree by temperature, very few are known to be activated by changes in temperature alone. To date, thermoTRPs are the only cation channels known to be activated by heat. Therefore, the heat-induced Ca^{2+} response of STIM1/Orai1 is not a common feature among ion channels and receptors.

Jurkat cells show CRAC channel-mediated heat off-response

We next tested the temperature responses of Jurkat T cells, a human T-cell line that expresses endogenous STIM1/Orai1-mediated CRAC channels. These cells also showed long-lasting heat off-responses of Ca^{2+} influx, with a τ value comparable to that of STIM1-overexpressing HeLa cells (433s and 380s, respectively) (Fig. 1d and Supplementary Fig. 1d). The off-response was ~44% of the store depletion-induced Ca^{2+} influx (Supplementary Fig. 2a), suggesting a relatively robust response. The response was blocked with Synta1 (Supplementary Fig. 2a and Fig. 1e), but not with ruthenium red (RR), a non-selective blocker of thermoTRPs (Supplementary Fig. 2b), indicating that CRAC channels rather than thermoTRPs mediate the temperature response of Jurkat T cells. The ET_{50} (the temperature to induce 50% of the maximal response) of the off-response was 38.8±0.6°C (Fig. 1e), indicating that the temperature response is within physiologically-relevant range. These results suggest that physiologically-relevant temperature variations can affect endogenous CRAC channels and induce Ca^{2+} influx.

Temperature shifts modify STIM1-dependent gene expression

Ca^{2+} influx through STIM1-dependent CRAC channels can activate NFAT, which functions together with the activator protein 1 (AP1), another transcription factor, to turn on gene expression in T cells28 (Fig. 2a). We examined the effect of temperature-induced Ca^{2+} influx on gene expression in a Jurkat cell line stably-expressing the NFAT-responsive luciferase reporter (containing both NFAT and AP1 binding sites in the promoter). Cells were pre-incubated at 37°C or 41°C before AP1 activation was induced by a saturating dose of phorbol 12-myristate 13-acetate (PMA, 1 μM) (Fig. 2b). The PMA-induced portion of the experiment was conducted at 37°C for both conditions, to avoid temperature-dependent modulation of transcriptional efficiency. Some NFAT-luciferase activity was observed in 37°C-pretreated cells with PMA compared to cells without PMA (Fig. 2c). Synta1 partially blocked the response (Fig. 2c, d) and the basal level of Ca^{2+} (Supplementary Fig. 2a), indicating that a constitutive CRAC channel activity at 37°C can contribute to slight NFAT activation. 41°C-pretreatment significantly increased the luciferase expression, and this increase was blocked by Synta1 (Fig. 2c, d). The Synta1-sensitive portion of luciferase

expression of 41°C-pretreated cells was 4.0±1.2 fold of that of 37°C-pretreated cells (Fig. 2d, right panel). Consistent with the effect of temperature shift on NFAT-luciferase expression, acutely heating the cells from 37°C to 41°C induced heat off-response of Ca^{2+} at 37°C (Supplementary Fig. 2c). These results suggest that heat off-response of Ca^{2+} through CRAC channels can independently activate NFAT-dependent transcription. However, the levels of NFAT induction are relatively small compared to induction via store depletion (Fig. 2c vs Fig. 2e).

Under physiological and pathophysiological conditions, the temperature effect might be more relevant in modulating store depletion-induced gene expression rather than temperature acting independently. We tested whether heat can modulate ionomycin (store depletion) induced SOCE and NFAT-dependent transcription. Indeed, 41°C-pretreatment increased ionomycin-induced Ca^{2+} influx measured at 37°C (Supplementary Fig. 2d) and enhanced the ionomycin/PMA-induced luciferase expression up to four-fold compared to that of 37°C treated cells (Fig. 2e, f and Supplementary Fig. 2e). Synta1 blocked ionomycin-induced luciferase expression (Fig. 2f). A significant increase in luciferase expression induced by 1 μM ionomycin/ 1 μM PMA was also observed in cells pretreated at 41°C for only 10 min (the minimal time period required for heating the cells to 41°C in these experiments) (Supplementary Fig. 2f) or at 39°C for 2 h (Supplementary Fig. 2g). Furthermore, we found that the luciferase activity induced by the OKT3 antibody (anti-human CD3) (which is an activator of T cell receptors and can cause ER Ca^{2+} store depletion) was significantly increased in the cells pretreated at 41°C (Supplementary Fig. 2h), demonstrating a general role of temperature shift in modulating store depletion-induced gene expression. As a control, we show that 41°C-pretreatment did not affect PMA-induced AP1-dependent luciferase expression in HEK293T cells transiently transfected with the AP1-luciferase reporter, demonstrating that not all transcriptional programs are significantly modulated by such a temperature pulse, and arguing for a specific role of heat on the Ca^{2+}-dependent NFAT pathway (Fig. 2g). We further subjected Jurkat cells to a 33°C-37°C-33°C temperature protocol (which could be experienced by circulating lymphocytes under physiological conditions), compared to 33°C control (Supplementary Fig. 2i). We observed a two-fold increase in NFAT-luciferase activity in samples pulsed at 37°C (Supplementary Fig. 2j). These results suggest that physiologically-relevant temperature variations have a significant effect on STIM1-dependent gene expression.

Heat induces STIM1 clustering without store depletion

We explored the underlying mechanism for temperature activation of STIM1. Similar to store depletion14, heating caused robust clustering (puncta formation) of GFP-STIM1 in HeLa cells (Fig. 3a–d and Supplementary Movie 1). The decay of the puncta closely followed the temperature decrease, but ~20% of the puncta were sustained after cooling back to 25°C (Fig. 3b–d). Simultaneous Ca^{2+} imaging revealed that the robust rise in intracellular Ca^{2+} occurred after cooling, when the clustering of STIM1 was partially diminished but had not returned to baseline (Fig. 3a–c). We further examined the temperature-dependence of STIM1 puncta formation at steady state temperatures and observed significantly increased puncta formation above 35°C. The ET_{50} of puncta formation was 43.6±1.2°C (Fig. 3e and see Figure legends for other parameters of the fit)

and the Q_{10} in the 37–43°C range was 6.8, which is well above the temperature sensitivity of most biological processes (Q_{10} of 2 to 3)29 and equivalent to temperature activation of some thermoTRPs such as TRPV330. These data suggests that STIM1 has a high degree of temperature-sensitivity.

We tested if STIM1 clustering occurs as an indirect consequence of heat causing store depletion, as suggested by a minor increase in Fura-2 signal observed during heating (Fig. 1b and Fig. 3a–c). We ruled out this possibility by showing that this minor Fura-2 signal is not due to Ca^{2+} depletion (Supplementary Fig. 3), but most likely due to the heat-sensitivity of the dye itself31,32. Nevertheless, we cannot rule out that subtle changes of ER Ca^{2+} levels (not detected in our assays) could play a minor role in the heat-induced STIM1 puncta formation. Another possibility is that heat induces STIM1 clustering via unfolding of the EF-hand and sterile-α-motif (SAM) of STIM1 (the mechanism shown to underlie store depletion-induced STIM1 clustering12,13) either directly or indirectly through heat affecting Ca^{2+} binding affinity of the EF-hand domain. Unfortunately, we are unable to directly test the involvement of the EF-SAM domain in heat-induced STIM1 puncta formation in vivo since the EF hand mutant STIM1-E87A constitutively forms puncta and mediates Ca^{2+} influx (See below Supplementary Fig. 5d and see10,11,13,33). However, in line with this possibility, in vitro analysis of the thermal stability of STIM1 EF-SAM domain estimated an ET_{50} of ~45°C in the presence of calcium34,35, which is comparable with ET_{50} of 43.6°C measured by heat-induced STIM1 puncta formation in HeLa cells in vivo (Fig. 3e).

The K-domain is required for heat-induced STIM1 clustering

Following its oligomerization, STIM1 translocates and clusters via mechanisms involving two protein domains: the polybasic domain (K-domain) and the CRAC-activating domain (CAD)16 [also known as the STIM1 Orai activating region (SOAR)15 or Orai1-activating small fragment (OASF)17]. The K-domain mediates STIM1 clustering through binding to an Orai1-independent target at ER-PM junctions, while CAD drives the process through direct CAD-Orai1 interaction16. We examined the roles of these critical domains in heat-induced STIM1 clustering by studying the deletion mutants: STIM1-deltaK (K-domain deleted) and STIM1-deltaCAD (CAD deleted). STIM1-deltaK itself cannot form store depletion-induced puncta, but Orai1 can rescue its puncta formation through CAD-Orai1 interaction14,16,36. As expected, after depleting ER Ca^{2+} stores with cyclopiazonic acid (CPA), we observed SOCE in STIM1-deltaK/Orai1 co-expressing cells (Fig. 4a, left panel). In contrast to STIM1/Orai1-transfected cells (Fig. 4a, b), these cells showed neither heat-induced puncta (Fig. 4c) nor heat off-responses (Fig. 4a, right panel). This implies that the K-domain is essential for heat-induced STIM1 puncta formation, and that the ability of Orai1 to rescue STIM1-deltaK function during store depletion does not occur during heat stimulation.

Since the STIM1-deltaK mutant retains store depletion-induced but lacks heat-induced Ca^{2+} influx when co-expressed with Orai1, it affords us the ability to investigate the role of heat-sensitivity of STIM1, without perturbing its activation via store depletion, on NFAT-dependent luciferase expression (Fig. 2). Consistent with Ca^{2+} influx results (Fig. 4a),

comparable ionomycin (100 nM) /PMA (1 μM)-induced NFAT-responsive luciferase activity was observed in HEK293T cells expressing either STIM1/Orai1 or STIM1-deltaK/Orai1 (Supplementary Fig. 4a, blue bars). In contrast, 41°C-pretreatment specifically enhanced the NFAT-luciferase activity only in cells transfected with STIM1/Orai1 (1.52 ± 0.06 fold, $p < 0.001$), but not in cells transfected with STIM1-deltaK/Orai1 (Supplementary Fig. 4a). Furthermore, STIM1/Orai1-expressing cells showed significantly higher basal Ca^{2+} level and NFAT-luciferase activity at 37°C compared to STIM1-deltaK/Orai1-expressing cells (Supplementary Fig. 4a, b), indicating that STIM1 temperature sensitivity may drive a basal level of Ca^{2+} influx and NFAT activation. The specific deficit in STIM1-deltaK to induce temperature-dependent transcriptional regulation suggests that temperature-sensitivity of STIM1 itself rather than any potential indirect effect of temperature on store depletion is responsible for the 41°C-incubation effects observed in Fig. 2.

CAD is critical for STIM1/Orai1 functional coupling15,16,17. Our results are in line with this since cells co-expressing STIM1-deltaCAD and Orai1 lost SOCE (Fig. 4a, left panel), heat off-responses (Fig. 4a, right panel), and NFAT-luciferase expression (Supplementary Fig. 4a). However, the STIM1-deltaCAD mutant was able to form heat-induced puncta (Supplementary Fig. 4c). This result suggests that the remaining K-domain in STIM1-deltaCAD may be sufficient to mediate heat-induced puncta, although STIM1-deltaCAD cannot functionally couple to Orai1. We further examined whether the entire carboxy-terminus of STIM1 (STIM1-ct), which contains both the K-domain and CAD, but lacks the amino-terminus of EF-hand and SAM domains, is sufficient to mediate the heat off-response. Some studies have shown that HEK293 cells co-transfected with STIM1-ct and Orai1 displayed constitutive Ca^{2+} influx36,37. However, such constitutive activity was not observed in STIM1-ct/Orai1-transfected HEK293T16, COS-7 cells38 or HeLa cells (Supplementary Fig. 4d, e). Consistent with a previous report37, 50 μM 2-APB elicited a small but significant increase in intracellular Ca^{2+} in STIM1-ct/Orai1-transfected HeLa cells, while inhibited the basal Ca^{2+} level in STIM1/Orai1-transfected cells (Supplementary Fig. 4d). STIM1-ct/Orai1-transfected HeLa cells failed to show heat off-responses (Supplementary Fig. 4e). These data suggest that the carboxy-terminal domain of STIM1 alone is not sufficient to induce the heat off-response, and that the amino-terminal EF-hand and SAM domains of STIM1 play a critical role in this process. However, since the STIM1-ct construct appears to be only marginally functional in our hands, the lack of heat off-responses with this construct could also be due to a sensitivity issue.

Heat blocks STIM1/Orai1 functional coupling

Ca^{2+} imaging is an indirect measurement of channel activity. We investigated membrane currents in whole-cell patch clamp experiments. Heat stimulation to 41–42°C of STIM1/Orai1-transfected HEK293T cells was followed by the activation of CRAC-like currents (Fig. 5a). The current density at −80 mV after temperature stimulation reached −12.6±2 pA/pF (n=12) compared to −3.7±1.3 pA/pF (n=16) for non-stimulated cells (Fig. 5b). Store depletion induced by CPA further increased the current to the same extent in both conditions (Fig. 5b). The inward rectifying current-voltage relationship, typical of I_{CRAC}, was similar for heat off-response and after store depletion (Fig. 5a, right panel). These results suggest that heat can induce STIM1/Ora1-mediated I_{CRAC} as a heat off-response.

If heating induces STIM1 puncta, why does the Orai1-mediated Ca^{2+} influx and current occur after cooling? To account for the heat off-response, we hypothesized that I_{CRAC} could be acutely blocked by heat. Indeed, I_{CRAC} pre-activated by CPA-induced store depletion was blocked by heating from 25°C to 42°C. The block is reversed by cooling back to 25°C (Fig. 5c). The temperature for half maximal block of I_{CRAC} is 36.9±0.9°C (n=9), and that for half maximal recovery is 36.9±1.3°C (n=6) (Fig. 5d). Similar results were obtained when testing the heat sensitivity of I_{CRAC} in the presence of external Ca^{2+} (Supplementary Fig. 5a, b). In addition, Ca^{2+} imaging studies confirmed that STIM1/Orai1-mediated SOCE (Supplementary Fig. 5c) and heat off-responses (Supplementary Fig. 1c) or E87A-STIM1/Orai1-mediated constitutive Ca^{2+} influx (Supplementary Fig. 5d) were blocked by high temperatures.

We asked if the heat-induced block of I_{CRAC} could be due to inhibition of CAD-Orai1 functional coupling by heat. To address this, we employed the GFP-STIM1-deltaK mutant since its puncta formation upon store depletion is mediated through interaction of CAD and Orai1. Similar to wild type STIM1, STIM1-deltaK and Orai1 mediated SOCE was also blocked by heat (Supplementary Fig. 5e). Heat did not disrupt the store depletion induced puncta of wild type STIM1 (Fig. 6a). This is presumably due to the ability of the existing K domain in mediating heat-induced puncta formation of wild type STIM1, independent of the CAD domain (as suggested by results shown in Supplementary Fig. 4c). Remarkably, the store depletion-induced STIM1-deltaK puncta was disrupted by heating the cells to 48°C (Fig. 6b). We further tested the hypothesis by examining the temperature response of HeLa cells co-transfected with CAD and Orai1. Consistent with previous reports15,16, cells co-transfected with CAD and Orai1 showed constitutive Ca^{2+} influx (Supplementary Fig. 5f). Importantly, this Ca^{2+} influx was suppressed by heating the cells to 42°C (Supplementary Fig. 5f), further supporting the hypothesis that heat can disrupt the functional coupling between CAD and Orai1. Together with the finding that Orai1 failed to rescue STIM1-deltaK function at high temperatures (see Fig. 4), these data suggest that heat can prevent or disrupt the coupling of STIM1 and Orai1 via the CAD. Collectively, our data suggests that although heat can induce STIM1 puncta, it cannot effectively activate Orai1 at high temperatures. Upon cooling, a portion of the STIM1 activity is sustained (Fig. 3d) and the functional coupling of STIM1/Orai1 is restored, resulting in the heat off-response.

Discussion

STIM1 has been established as the ER Ca^{2+} sensor of SOCE8. Here we report that STIM1 is activated by physiologically-relevant temperatures independently of store depletion (Fig. 3), and that the temperature sensitivity of STIM1-dependent Ca^{2+} signaling can impact gene expression in immune cells in response to heat alone, or in modulating store depletion-induced signaling (Fig. 2). Interestingly, STIM1 was recently shown to be directly activated via S-glutathionylation under conditions of oxidative stress, proposing that STIM1 is a redox sensor39. Therefore, STIM1 could function as a polymodal sensor of temperature, ER Ca^{2+}, and oxidative stress. Mechanistically, unfolding of the STIM1 EF-SAM domain upon ER Ca^{2+} depletion is thought to be the initiating event of STIM1 activation12,13. In vitro studies have shown that heat is an effective way to denature the EF-SAM domain34,35. It has also been postulated that S-glutathionylation of a cystein residue near the EF-SAM

domain may result in a similar unfolding effect39. Therefore, all of these different stimuli may share a similar mechanism for initiating STIM1 activation, providing a mechanistic basis for STIM1 to function as a polymodal sensor.

Temperature, however, has more complicated effects on subsequent events of STIM1/Orai1 activation. Heat induces STIM1 clustering but inhibits STIM1-Orai1 functional coupling. This is due to different effects of temperature on distinct domains of STIM1: elevated temperatures can potentially enhance the K domain-mediated targeting, while prevent / disrupt CAD-Orai1 interaction. This complexity allows temperature-dependent heat off-response, but also offers fine-tuning of CRAC channel activity. Indeed, we observed a STIM1/Orai1-mediated basal/constitutive Ca^{2+} influx at 37°C, which appears to depend on STIM1 temperature sensitivity (Supplementary Fig. 4b). In addition, we observed profound temperature effects on store depletion-induced transcriptional activation (Fig. 2e, f).

The identification of STIM1/Orai1 as a novel temperature-activated cation channel is exceptional. Although most proteins are somewhat temperature-sensitive (Q_{10} of 2 to 3), very few are specifically activated by change in temperature within the physiological range40. In contrast, STIM1-clustering (Q_{10} = 7) and STIM1/Orai1-mediated Ca^{2+} off-response are highly temperature-dependent, resulting in a dramatic effect of temperature on NFAT-dependent gene expression. Thus STIM1/Orai1 comprises a novel family of temperature-activated cation channel other than thermoTRPs. Sensing temperature is essential for organism survival and efficient metabolism. It has been demonstrated that thermoTRPs expressed in somatosensory neurons play important roles in thermosensation and nociception23,24. Less is known about molecular mechanisms of temperature sensation in other cell types exposed to significant temperature shifts such as immune cells. Immune cells can experience temperature variations while circulating between central (37°C or up to 41°C at normal or febrile conditions, respectively) and peripheral tissues (33°C or up to 37°C at normal or febrile conditions, respectively) or under conditions of hypothermia, hyperthermia. The observation that temperature-induced STIM1/Orai1 activation can lead to Ca^{2+} influx and impact gene expression in Jurkat T cells suggests that STIM1 could serve as a molecular temperature sensor of immune cells. Pre-exposure of Jurkat T cells to high temperatures which can activate STIM1 but prevent Orai1 channel opening promoted subsequent STIM1/Orai1-mediated Ca^{2+} signaling and gene expression when the cells were shifted to lower temperatures (Fig. 2). We therefore speculate that STIM1/Orai1-mediated temperature sensing in immune cells may provide a priming mechanism for these cells to function at peripheral sites where they are usually engaged in immune responses (e.g. peripheral tissue injury), but the temperature is suboptimal (below 37 °C) under normal conditions of body temperature. In the situation of fever, this mechanism could be a benefit not only for immune responses at peripheral locations during fever but also for overall immune responses after fever. Future studies will explore the in vivo consequence of STIM1 temperature sensitivity in immune cells under both normal and febrile conditions.

STIM1/Orai1-dependent SOCE is also observed in a wide variety of other cell types including platelets41, skeletal muscles42, and keratinocytes43. STIM1 temperature sensitivity could be of physiological relevance to those cells as well. For example, platelets express abundant STIM1/Orai1, and rely on STIM1/Orai1-mediated Ca^{2+} influx for their

function44. Like immune cells, they can experience dramatic temperature variations while circulating between central and peripheral locations of the body. In addition, STIM1-mediated SOCE has been proposed to play a critical role for the development, contraction, fatigue, and remodeling of skeletal muscle cells42. The temperature of skeletal muscle can increase from 33°C up to 39°C during exercise45, raising the possibility that heat-induced Ca^{2+} influx via STIM1 could play a role in skeletal muscle physiology. Keratinocytes experience wide temperature variations and are implicated in thermosensation23. STIM1-deficient mice die perinatally, and future analysis of mice specifically lacking STIM1 in various tissues will help determine the physiological role of STIM1 thermosensitivity.

Methods

Clones and reagents

See Supplementary Methods for detailed description of the clones and reagents used in the study.

Cell culture and transient transfection

Conditions for culturing HeLa or HEK293T cells were as same as those described previously46 and see Supplementary Methods for more detailed description.

Fluorometric imaging plate reader (FLIPR)

FLIPR experiments with adherent cells were performed essentially as described previously47. The temperature change of the medium inside the well was controlled by a custom-designed temperature-control device as described47. For non-adherent Jurkat cells, we alternatively employed the no-wash FLIPR Calcium 4 Assay Kit (Molecular Device) to avoid steps of washing and spinning. See Supplementary Methods for more detailed description. The initial drop of Fluo-3 or Calcium 4 fluorescent signal during heating is always observed regardless of cell types and whether cells are transfected (Fig. 1d and Supplementary Fig. 1a, b, c, j and Supplementary Fig. 2a–c). Currently, we do not totally understand the exact nature of this drop. It could be mediated by multiple factors including temperature quench of Fluo-3 fluorescence, heat inhibition of Ca^{2+} influx and heat facilitation of Ca^{2+} removal from the cytosol.

Fura-2 single cell Ca^{2+} imaging

Transfected cells grown on coverslips were loaded with ratiometric Ca^{2+} indicator dye Fura-2 (Molecular Probes) in the Ca^{2+} imaging buffer [1 × Hanks Balanced Salt Solution (HBSS, 1.3 mM Ca^{2+}) supplemented with 10 mM HEPES] for 30 min at RT and then subject to imaging on an inverted Zeiss Axiovert 200M microscope with a 20× Fluar objective (N.A.: 0.75). For measuring tonic basal Ca^{2+} level at 37°C shown in Supplementary Fig. 4b, cells gown at 37°C were loaded with Fura-2, washed and assayed at 37°C. The intracellular Ca^{2+} concentration was expressed as the 340/380 ratio. A separate set of experiments were performed in order to convert the heat off-response of Fura-2 ratio at 25°C to Ca^{2+} concentration according to the method described in the Supplementary Methods. The temperature change of the bath solution was controlled using a CL-100 temperature controller (Warner Instruments) and a SC-20 Solution In-Line Heater/Cooler

(Harvard Apparatus). Temperature of the bath solution was recorded with a thermistor placed at the outlet of the perfusion.

NFAT-luciferase assay and AP-1-luciferase assay

See the Supplementary Methods for detailed description of the luciferase assay.

GFP-STIM1 puncta measurement and analysis

HeLa cells grown on 12-mm round coverslips were transfected with 0.2 μg of GFP-hSTIM1 DNA. 18–24 h after transfection, cells were loaded with Fura-2 and subjected to live-cell imaging of GFP and Fura-2 simultaneously on an inverted Zeiss Axiovert 200M microscope with a 20× Fluar objective (N.A.: 0.75) and 2.5× Optovar (total 50× magnification). Each frame of images was collected about every 8 s. Heating and cooling the bath solution during the continuous recording caused changes in focus (potentially due to expansion and contraction of the glass coverslips) and thus required a manual refocus. GFP images collected during the re-focusing period were excluded from puncta analysis as indicated in Fig. 3b, c.

To quantitatively analyze heat-induced GFP-STIM1 puncta, GFP images were processed using the convolve filter, adjusted with the threshold function (intensity ≥ mean of background intensity + 3 × standard deviation), and followed by the analyze particle function (particles size ≥ 10 pixel^2; circularity: 0.4–0.8) using the ImageJ software (National Institute of Health). Supplementary Movie 1 was built from GFP and Fura-2 340/380 ratio images using MetaMorph software (Molecular Devices). The movies play images at a frame rate of 0.2 s.

In Fig. 3e, in order to measure the temperature dependence of STIM1 puncta formation at steady state temperatures, temperature was sequentially stepped from 25°C to 29°C, 35°C, 37°C, 39°C, 41°C, 43°C, and 50°C (cells were held at each temperature point for about 2 min to allow steady state evaluation of puncta formation). GFP images were continuously recorded and puncta were quantitatively analyzed as described above. Puncta formed during the last 30s at each temperature point (which represents steady state puncta) were averaged and used to generate the data shown in Fig. 3e.

Confocal microscopy

In Fig. 4b–c, Supplementary Fig. 4c and Fig. 6a, b, transfected HeLa cells grown on 12-mm round coverslips were mounted to an Olympus Fluoview FV500 LSM microscope and continuously perfused with the indicated buffers shown in the Figures. To better appreciate the translocation and puncta formation of the constructs, GFP images were taken with a 60× water dipping objective (N.A.: 0.90) using the Z-stack module at either 25 °C or after the temperature was ramped to 48 °C. For imaging store depletion induced puncta, cells were perfused with the buffer containing 0 mM Ca^{2+}, 1mM EGTA and 1 μM Tg for 10 min prior to taking images. Images were analyzed using ImageJ software.

Q_{10} calculation

The Q_{10} value (i.e. the proportional change in response per 10°C change in temperature) was calculated using the equation $Q_{10} = 10^{[(\text{regression slope}).10]}$, where the regression slope is the slope of the linear fit of Log (response) versus temperature plot.

Electrophysiology

HEK293T cells over-expressing GFP-STIM1 and Orai1 were subject to patch-clamp experiments in standard whole-cell recordings. Pipettes were filled with (mM): 120 Cs Methanesulfonate, 10 HEPES, 10 $MgCl_2$, 4 EGTA and 2 $CaCl_2$, pH 7.3 with CsOH. The final Ca^{2+} concentration was ~175 nM free Ca^{2+} as determined using Maxchelator software; this prevents passive store depletion of the internal Ca^{2+} stores. See Supplementary Information for external solutions, recording protocols and analysis methods.

Data Analysis

Data in all figures are shown as mean ± SEM. Statistical significance was evaluated using either unpaired Student's *t*-test for comparing difference between two samples or one way ANOVA for comparing three or more samples. * $p < 0.05$, ** $p < 0.01$, *** $p < 0.001$.

Supplementary Material

Refer to Web version on PubMed Central for supplementary material.

Acknowledgements

We thank Drs. R. Y. Tsien, P. Shultz, S-S Tian, A. Parker, D. Tully and S.F. Pan for providing reagents; E. Rodrigo, E. Peters, J. Liu, K. Spencer, T. Earley, D. Li, and J. Mitsios for experimental help; M. Schmidt for providing advice on GFP-STIM1 puncta analysis; C. Shmedt, M. Cooke, D. Geurini, S-S. Tian and S. Sanford for discussions; and N. Hong and J. Grandl for reading the manuscript. This research was supported by NIH grants DE016927, NS046303 and by the Novartis Research Foundation. B.X. is the postdoctoral fellowship recipient from Canadian Institutes of Health Research, Alberta Heritage Foundation for Medical Research and American Heart Association. B.C. is the postdoctoral fellowship recipient from American Heart Association.

References

1. Parekh AB, Putney JW Jr. Store-operated calcium channels. Physiol Rev. 2005; 85:757–810. [PubMed: 15788710]
2. Hogan PG, Lewis RS, Rao A. Molecular basis of calcium signaling in lymphocytes: STIM and ORAI. Annu Rev Immunol. 2010; 28:491–533. [PubMed: 20307213]
3. Oh-hora M, Rao A. Calcium signaling in lymphocytes. Curr Opin Immunol. 2008; 20:250–258. [PubMed: 18515054]
4. Vig M, Kinet JP. Calcium signaling in immune cells. Nat Immunol. 2009; 10:21–27. [PubMed: 19088738]
5. Feske S, Picard C, Fischer A. Immunodeficiency due to mutations in ORAI1 and STIM1. Clin Immunol. 2010; 135:169–182. [PubMed: 20189884]
6. Putney JW Jr. A model for receptor-regulated calcium entry. Cell Calcium. 1986; 7:1–12. [PubMed: 2420465]
7. Lewis RS. The molecular choreography of a store-operated calcium channel. Nature. 2007; 446:284–287. [PubMed: 17361175]
8. Cahalan MD. STIMulating store-operated Ca(2+) entry. Nat Cell Biol. 2009; 11:669–677. [PubMed: 19488056]

9. Roos J, et al. STIM1, an essential and conserved component of store-operated Ca2+ channel function. J Cell Biol. 2005; 169:435–445. [PubMed: 15866891]
10. Liou J, et al. STIM is a Ca2+ sensor essential for Ca2+-store-depletion-triggered Ca2+ influx. Curr Biol. 2005; 15:1235–1241. [PubMed: 16005298]
11. Zhang SL, et al. STIM1 is a Ca2+ sensor that activates CRAC channels and migrates from the Ca2+ store to the plasma membrane. Nature. 2005; 437:902–905. [PubMed: 16208375]
12. Luik RM, Wang B, Prakriya M, Wu MM, Lewis RS. Oligomerization of STIM1 couples ER calcium depletion to CRAC channel activation. Nature. 2008; 454:538–542. [PubMed: 18596693]
13. Stathopulos PB, Zheng L, Li GY, Plevin MJ, Ikura M. Structural and mechanistic insights into STIM1-mediated initiation of store-operated calcium entry. Cell. 2008; 135:110–122. [PubMed: 18854159]
14. Liou J, Fivaz M, Inoue T, Meyer T. Live-cell imaging reveals sequential oligomerization and local plasma membrane targeting of stromal interaction molecule 1 after Ca2+ store depletion. Proc Natl Acad Sci U S A. 2007; 104:9301–9306. [PubMed: 17517596]
15. Yuan JP, et al. SOAR and the polybasic STIM1 domains gate and regulate Orai channels. Nat Cell Biol. 2009; 11:337–343. [PubMed: 19182790]
16. Park CY, et al. STIM1 clusters and activates CRAC channels via direct binding of a cytosolic domain to Orai1. Cell. 2009; 136:876–890. [PubMed: 19249086]
17. Muik M, et al. A Cytosolic Homomerization and a Modulatory Domain within STIM1 C Terminus Determine Coupling to ORAI1 Channels. J Biol Chem. 2009; 284:8421–8426. [PubMed: 19189966]
18. Lederman HM, Brill CR, Murphy PA. Interleukin 1-driven secretion of interleukin 2 is highly temperature-dependent. J Immunol. 1987; 138:3808–3811. [PubMed: 3495573]
19. Hanson DF, Murphy PA, Silicano R, Shin HS. The effect of temperature on the activation of thymocytes by interleukins I and II. J Immunol. 1983; 130:216–221. [PubMed: 6600177]
20. Hanson DF. Fever and the immune response. The effects of physiological temperatures on primary murine splenic T-cell responses in vitro. J Immunol. 1993; 151:436–448. [PubMed: 8326136]
21. Gern JE, Jayman JR, Goldberg LI, Murphy PA, Lederman HM. Temperature is a powerful promoter of interleukin 2 transcription. Cytokine. 1991; 3:389–397. [PubMed: 1751776]
22. Hanson DF. Fever, temperature, and the immune response. Ann N Y Acad Sci. 1997; 813:453–464. [PubMed: 9100921]
23. Dhaka A, Viswanath V, Patapoutian A. Trp ion channels and temperature sensation. Annu Rev Neurosci. 2006; 29:135–161. [PubMed: 16776582]
24. Basbaum AI, Bautista DM, Scherrer G, Julius D. Cellular and molecular mechanisms of pain. Cell. 2009; 139:267–284. [PubMed: 19837031]
25. Yuan JP, Zeng W, Huang GN, Worley PF, Muallem S. STIM1 heteromultimerizes TRPC channels to determine their function as storeoperated channels. Nat Cell Biol. 2007; 9:636–645. [PubMed: 17486119]
26. DeHaven WI, et al. TRPC channels function independently of STIM1 and Orai1. J Physiol. 2009; 587:2275–2298. [PubMed: 19332491]
27. Sun L, Chen S, Jiang J, Xie Y, Yu C. Conpounds for infammation and immune-related uses. 2006 Aug 8. WO/2006/081391.
28. Oh-Hora M, et al. Dual functions for the endoplasmic reticulum calcium sensors STIM1 and STIM2 in T cell activation and tolerance. Nat Immunol. 2008; 9:432–443. [PubMed: 18327260]
29. Moran U, Phillips R, Milo R. SnapShot: key numbers in biology. Cell. 2010; 141:1262–1262. e1261. [PubMed: 20603006]
30. Peier AM, et al. A heat-sensitive TRP channel expressed in keratinocytes. Science. 2002; 296:2046–2049. [PubMed: 12016205]
31. Paltauf-Doburzynska J, Graier WF. Temperature dependence of agonist-stimulated Ca2+ signaling in cultured endothelial cells. Cell Calcium. 1997; 21:43–51. [PubMed: 9056076]
32. Oliver AE, Baker GA, Fugate RD, Tablin F, Crowe JH. Effects of temperature on calcium-sensitive fluorescent probes. Biophys J. 2000; 78:2116–2126. [PubMed: 10733989]

33. Mercer JC, et al. Large store-operated calcium selective currents due to co-expression of Orai1 or Orai2 with the intracellular calcium sensor, Stim1. J Biol Chem. 2006; 281:24979–24990. [PubMed: 16807233]
34. Stathopulos PB, Li GY, Plevin MJ, Ames JB, Ikura M. Stored Ca2+ depletion-induced oligomerization of stromal interaction molecule 1 (STIM1) via the EF-SAM region: An initiation mechanism for capacitive Ca2+ entry. J Biol Chem. 2006; 281:35855–35862. [PubMed: 17020874]
35. Zheng L, Stathopulos PB, Li GY, Ikura M. Biophysical characterization of the EF-hand and SAM domain containing Ca2+ sensory region of STIM1 and STIM2. Biochem Biophys Res Commun. 2008; 369:240–246. [PubMed: 18166150]
36. Huang GN, et al. STIM1 carboxyl-terminus activates native SOC, I(crac) and TRPC1 channels. Nat Cell Biol. 2006; 8:1003–1010. [PubMed: 16906149]
37. Wang Y, et al. STIM protein coupling in the activation of Orai channels. Proc Natl Acad Sci U S A. 2009; 106:7391–7396. [PubMed: 19376967]
38. Korzeniowski MK, Manjarres IM, Varnai P, Balla T. Activation of STIM1-Orai1 involves an intramolecular switching mechanism. Sci Signal. 2010; 3:ra82. [PubMed: 21081754]
39. Hawkins BJ, et al. S-glutathionylation activates STIM1 and alters mitochondrial homeostasis. J Cell Biol. 2010; 190:391–405. [PubMed: 20679432]
40. Bandell M, Macpherson LJ, Patapoutian A. From chills to chilis: mechanisms for thermosensation and chemesthesis via thermoTRPs. Curr Opin Neurobiol. 2007; 17:490–497. [PubMed: 17706410]
41. Varga-Szabo D, Braun A, Nieswandt B. Calcium signaling in platelets. J Thromb Haemost. 2009; 7:1057–1066. [PubMed: 19422456]
42. Stiber J, et al. STIM1 signalling controls store-operated calcium entry required for development and contractile function in skeletal muscle. Nat Cell Biol. 2008; 10:688–697. [PubMed: 18488020]
43. Gwack Y, et al. Hair loss and defective T- and B-cell function in mice lacking ORAI1. Mol Cell Biol. 2008; 28:5209–5222. [PubMed: 18591248]
44. Varga-Szabo D, et al. The calcium sensor STIM1 is an essential mediator of arterial thrombosis and ischemic brain infarction. J Exp Med. 2008; 205:1583–1591. [PubMed: 18559454]
45. Kenny GP, et al. Muscle temperature transients before, during, and after exercise measured using an intramuscular multisensor probe. J Appl Physiol. 2003; 94:2350–2357. [PubMed: 12598487]
46. Xiao B, et al. Identification of transmembrane domain 5 as a critical molecular determinant of menthol sensitivity in mammalian TRPA1 channels. J Neurosci. 2008; 28:9640–9651. [PubMed: 18815250]
47. Grandl J, et al. Pore region of TRPV3 ion channel is specifically required for heat activation. Nat Neurosci. 2008; 11:1007–1013. [PubMed: 19160498]

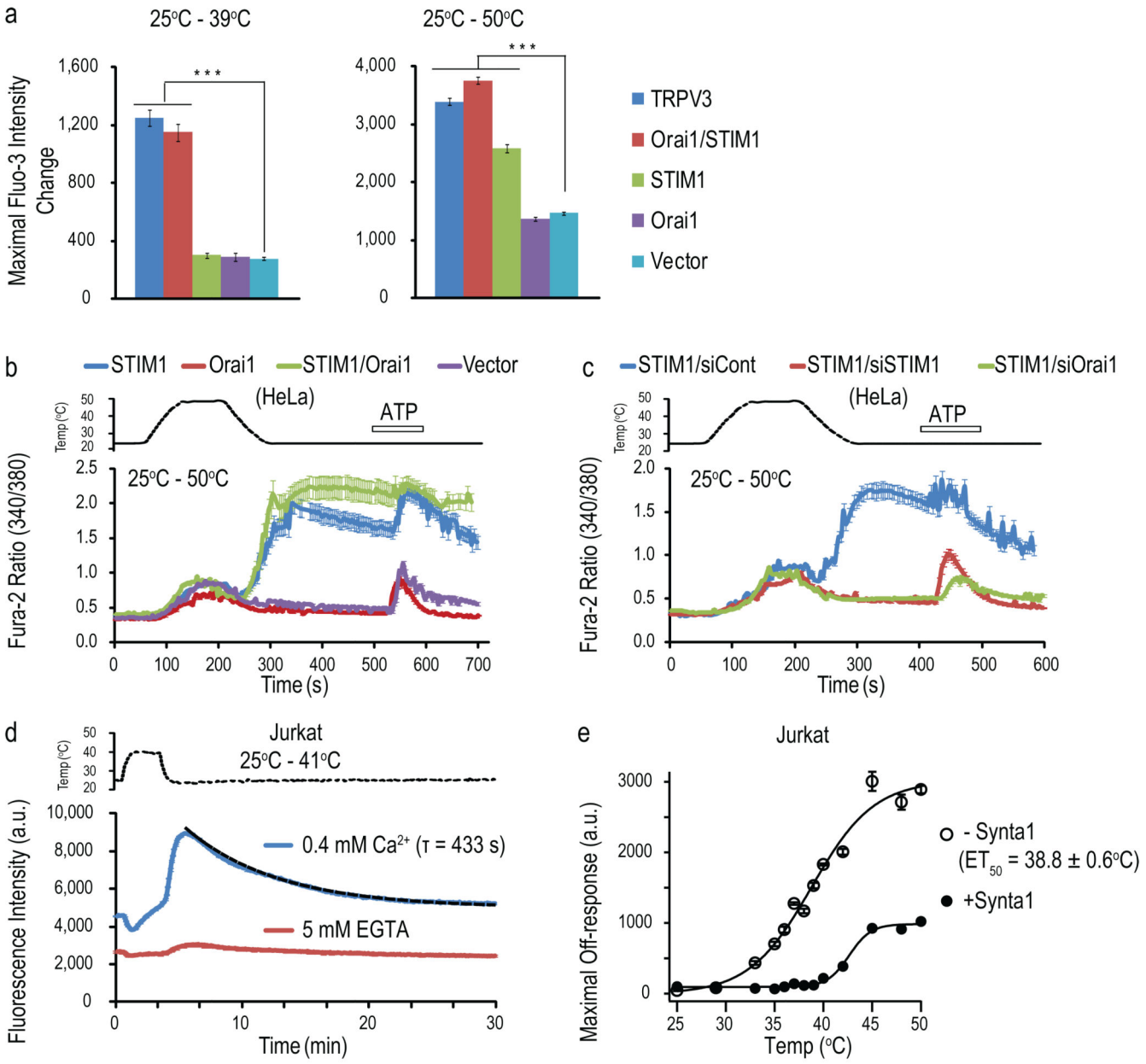

Fig. 1. STIM1/Orai1-mediated Ca^{2+} influx in response to heating

(a) Maximal fluorescence intensity changes of HEK293T cells transfected with various DNA constructs evoked by the temperature stimulation (n=5, ***p<0.001, one way ANOVA). (b,c) Fura-2 ratiometric single cell calcium imaging of HeLa cells transfected with various DNA constructs (b), and co-transfected with GFP-STIM1 and the indicated siRNAs (c) in response to a heating pulse to ~50°C. 100 μM ATP was applied at the end as a control for cell viability. (d) Temperature responses to a heating pulse to 41°C of Jurkat cells assayed on FLIPR with or without extracellular Ca^{2+}. The black dashed line represents fit with a mono-exponential function and the τ value of this fit was given to illustrate the overall kinetics of the Ca^{2+} signal decay of the heat off-response. (e) Temperature-dependent off-responses of Jurkat cells assayed on FLIPR with or without 20 μM Synta1

and fitted with Boltzmann equations. Cells were heated from 25°C to the indicated various temperatures and then cooled back to 25°C for assaying the heat off-response. (data shown as mean ± SEM.)

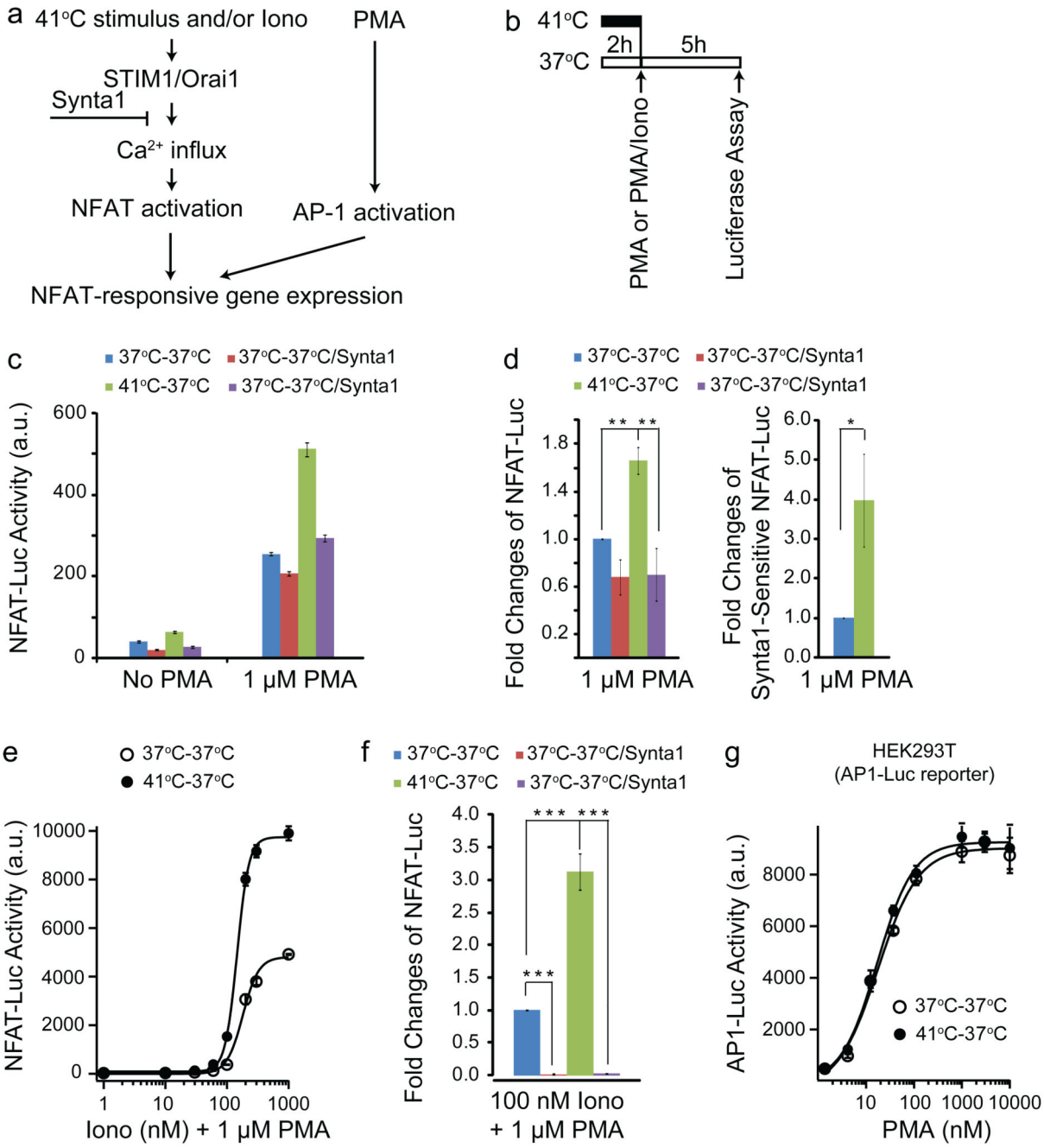

Fig. 2. Temperature effects on CRAC channel-dependent gene expression

(a) Schematic illustration of NFAT-responsive gene expression system. (b) Protocol used for assaying temperature effects on NFAT-responsive or AP1-responsive luciferase expression. (c) Representative experiment showing luciferase activity of Jurkat-NFAT-Luc cells with the indicated treatment conditions. (d) Fold changes of NFAT-luciferase activity before (left panel) or after (right panel) subtracting Synta1-insensitive portion of the responses [averaged from five separate experiments represented in (c) and normalized to the responses of 37°C-treated cells.]. (e) Representative experiment showing concentration-dependent

responses of ionomycin-induced NFAT-luciferase activity under the indicated treatment conditions and fitted with Hill equations. (f) Average fold changes of 100 nM ionomycin/1 μM PMA-induced NFAT-luciferase activity under the indicated conditions (averaged from six separate experiments). (g) Concentration-dependent responses of PMA-induced AP1-dependent luciferase activity in HEK293T cells transfected with the AP1-Luc reporter fitted with Hill equations. (data shown as mean ± SEM, *$p < 0.05$, **$p < 0.01$, ***$p < 0.001$)

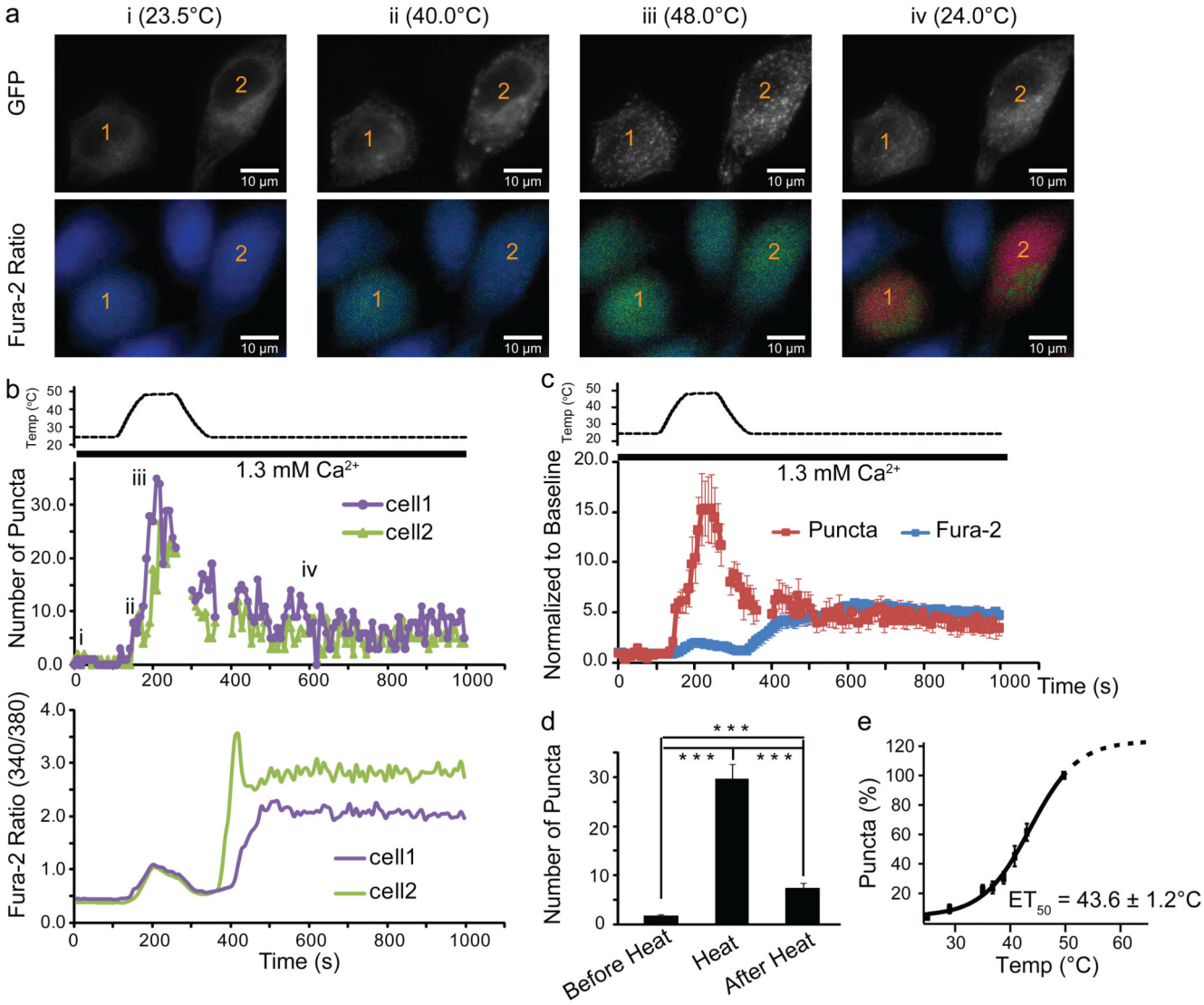

Fig. 3. Heat-induced STIM1 clustering

(a) Images of GFP and Fura-2 ratio from two representative GFP-STIM1-transfected HeLa cells before (i), during (ii and iii) and after heating (iv). (b) Temperature-dependent changes of GFP-STIM1 puncta and Fura-2 signal of the 2 individual cells labeled in (a). i, ii, iii, iv indicates the time points at which the images shown in (a) were taken. (c) Average temperature-dependent changes of GFP-STIM1 puncta (red trace) and Fura-2 Ca^{2+} imaging signal (blue trace) (average of 14 cells). Gaps in panel (b and c) indicate the times at which focus was changed due to the heating and cooling process (see Methods). (d) Average number of puncta before, upon, and 10 min after heating (33 cells from 5 separate experiments, ***$p < 0.001$). (e) Temperature-dependence of STIM1 puncta formation at steady state temperatures fitted with a Boltzmann equation (see Methods) (27 cells from 4 separate experiments). It should be noted that heat-induced STIM1 puncta formation may not reach saturation at 50°C although the value at 50°C was used for normalization as 100%. Using a Boltzmann equation without any constrains, the parameters obtained from the fit

are: baseline = 4.5±3.0%, maximum=118.8±15.7%, ET_{50}=43.6±1.2, slope=4.3±0.8. (data shown as mean ± SEM)

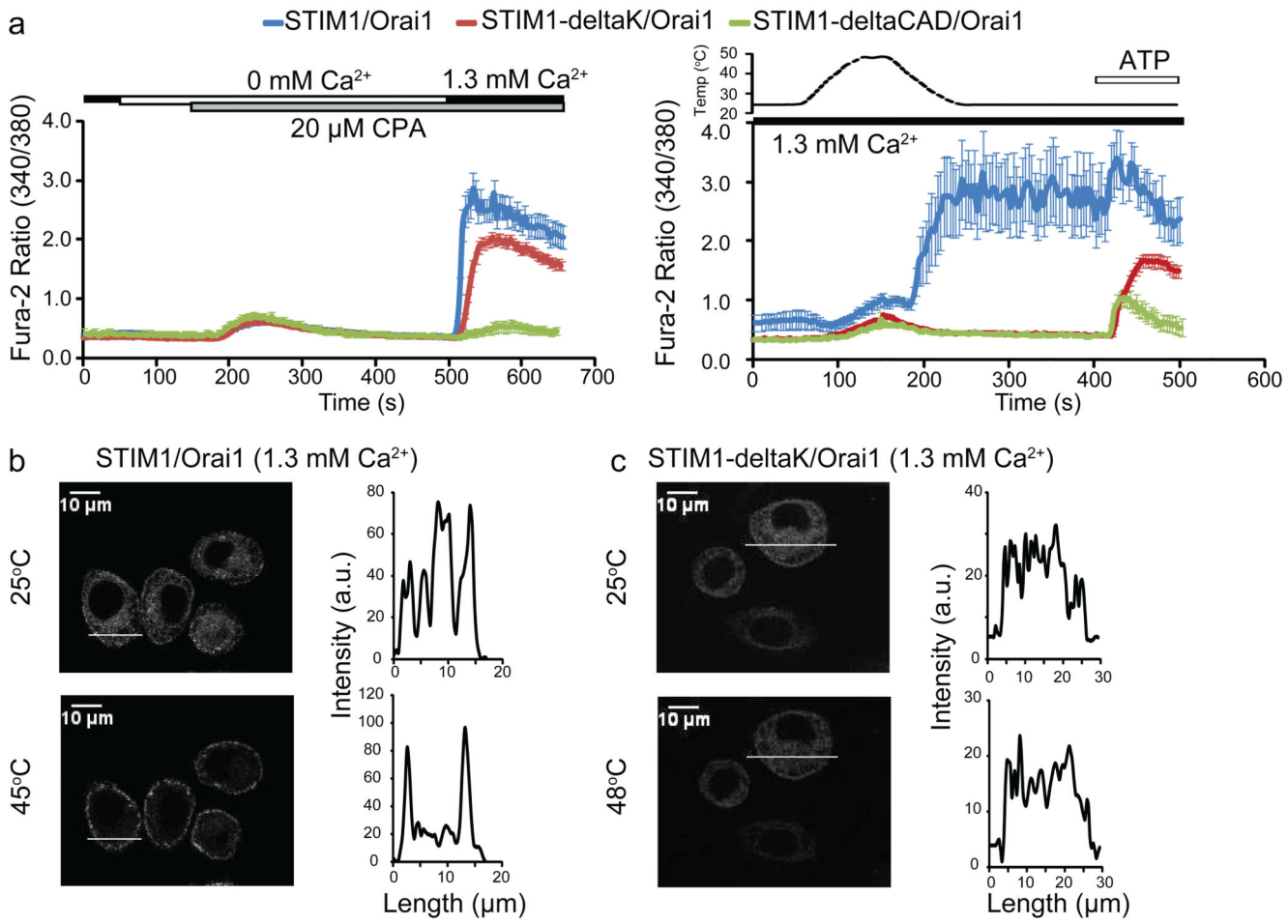

Fig. 4. The STIM1 K-domain is essential for heat-induced STIM1 clustering

(a) CPA-induced store depletion and SOCE (left panel) or temperature responses (right panel) of HeLa cells transfected with the indicated constructs. (b–c) Confocal analysis of HeLa cells co-transfected with Orai1 and the indicated constructs at 25°C (upper panels) or after heating to the indicated temperatures (lower panels). GFP intensity plots represent localization of each construct across the cell as indicated by the white line.

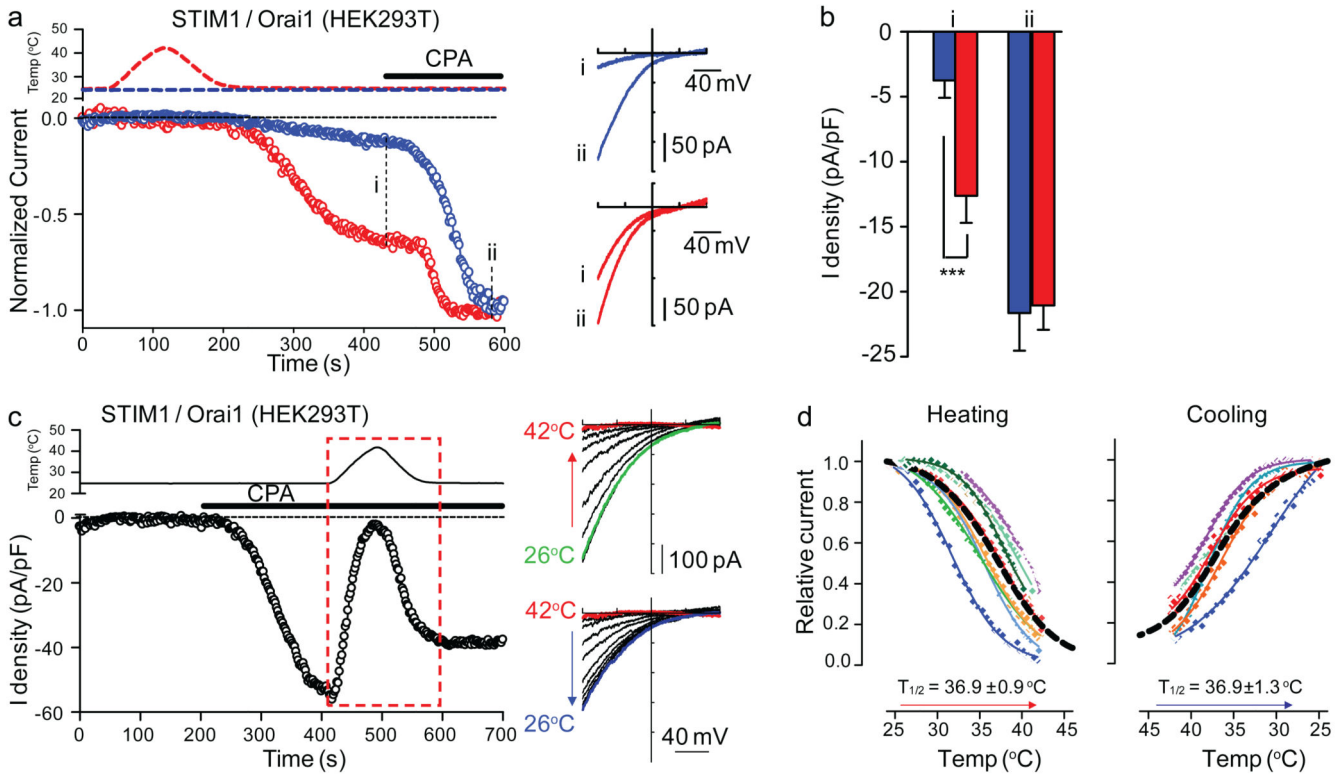

Fig. 5. Temperature effects on STIM1/Orai1-mediated I_{CRAC} and STIM1/Orai1 functional coupling

(a) Left panel: Time courses of the normalized currents recorded at −80 mV without (blue) or with (red) temperature stimulation. Perfusion of 10 μM CPA is indicated. Right panel: I–V curves from the same recordings shown on the left panel at the indicated time points (i, ii). (b) Average current density of control (blue, n=16) or temperature-stimulated cells (red, n=12) at the indicated time points (i, ii) (*** $p < 0.001$, unpaired t test). (c) Left panel: Time course of the current recorded at −80 mV in response to the indicated stimuli. Right panels: I–V curves at 10 second intervals from recordings during the heating phase (upper panel) and cooling phase (lower panel) of the temperature stimulus (red box in left panel). (d) Current-temperature relationships of I_{CRAC} at −80 mV during heating (left, n = 9) or cooling (right, n = 6) fitted with a Boltzmann equation. The black dashed line is the average fit. $T_{1/2}$ is the average value of individual $T_{1/2}$ determined for each cell. The cells were dialyzed with a pipette solution containing ~175 nM free Ca^{2+} and external solution containing either 2.5 mM Ca^{2+} (a, b) or no divalent cations (c, d). (data shown as mean ± SEM)

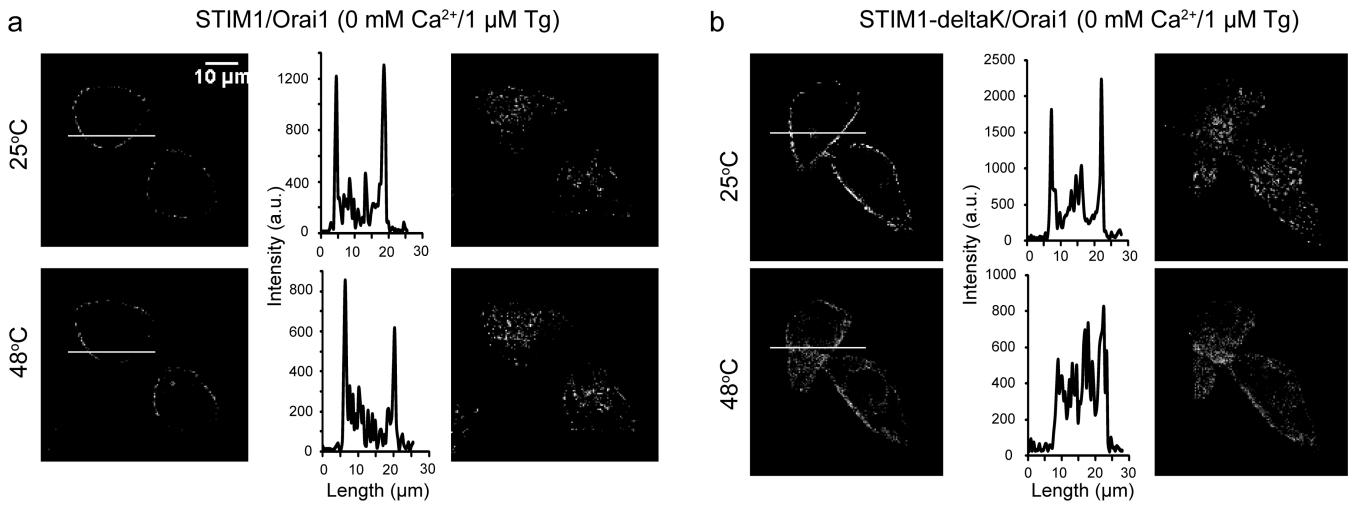

Fig. 6. Heat disrupts store depletion-induced puncta in GFP-STIM1-deltaK/Orai1 co-transfected HeLa cells

(a–b) Confocal analysis of HeLa cells co-transfected with Orai1 and either GFP-STIM1 (a) or GFP-STIM1-deltaK (b) under store-depleted conditions (0mM Ca^{2+}/1 μM Tg), at 25 °C (upper panels) or after heating to 48 °C (lower panels). Left panels: Confocal images of mid-section of cells. Middle panels: GFP intensity plots represent localization of each construct across the cell as indicated by the white line in the left panel. Right panels: Confocal images of lower-section (cell footprint) of the same cells shown in left panels.